minerals

MDPI

Article

Study of a Novel Fluidized Bed Flotation Column with Enhanced Bubble Dispersion

Mao Yin [1,2,*], Ning Han [1], Ting Yang [1] and Yanfeng Li [1]

[1] School of Chemical Engineering and Technology, China University of Mining and Technology, Xuzhou 221116, China; 15651462381@163.com (N.H.); ts22040189p31@cumt.edu.cn (T.Y.); lyf3344@126.com (Y.L.)
[2] Henan SUNHO Group Company Limited, Shangqiu 476600, China
* Correspondence: tb23040018a41@cumt.edu.cn

Abstract: Flotation machines and flotation columns are widely used as separation equipment for coal sludge. In order to obtain better flotation results for different particle sizes, the bubble distribution and size in the flow field need to be studied. In this paper, a novel three-phase fluidized bed flotation column (TFC) was designed, and the shear effect of liquid velocity (0.198 m/s, 0.226 m/s, and 0.254 m/s) and static bed height (0.1 m, 0.2 m, and 0.3 m) on the bubbles in the mineralized flow field region was investigated and evaluated for the formation of bubbles by shear in laboratory and semi-industrial experiments. The results show that the increase in filling bed height has a very obvious strengthening effect on the reduction of bubble diameter, and after the filling bed height reaches a certain value, the filling bed height will weaken the effect of apparent gas velocity on bubble diameter. The apparent gas velocity has different influencing effects on bubble diameter, and under conditions of low water velocity, the increase in the apparent gas velocity contributes to the reduction of bubble diameter. The conclusions of this study are expected to optimize the operating parameters of the flotation mineralization process and enrich the study of TFC, which can provide a reference for the design of future TFC studies.

Keywords: flotation column; bubbles; liquid velocity; bed height; operating parameters

Citation: Yin, M.; Han, N.; Yang, T.; Li, Y. Study of a Novel Fluidized Bed Flotation Column with Enhanced Bubble Dispersion. *Minerals* **2024**, *14*, 84. https://doi.org/10.3390/min14010084

Academic Editor: Luis Vinnett

Received: 22 December 2023
Revised: 6 January 2024
Accepted: 8 January 2024
Published: 11 January 2024

1. Introduction

A gas-liquid-solid three-phase fluidized bed flotation column defined in this study is a solid particle bed fluidized by compressed air flowing in parallel upward as the dispersed gas phase and water as the continuous liquid phase. Reese et al. [1] discussed the industrial applications of three-phase fluidized bed systems. The advantages of a three-phase fluidized bed system have been widely used in research involving chemistry, physics, and biochemistry [2,3]. The advantages of three-phase fluidized beds have been widely used in the fields of chemistry, physics, and biochemistry. Since the invention of the flotation column, it has made great progress because of its wide adaptability in handling fine-grained materials and other scientific fields [4–8]. The gas parameters, such as gas retention rate, bubble diameter, and bubble surface area flux, are the most critical indexes to evaluate flotation, which directly affect the effectiveness of flotation columns [9–11]. Therefore, when controlling and diagnosing the operation of flotation columns, it is important to know the gas parameters. There have been many articles related to gas parameters in the literature [12–16]. The research on gas parameters in flotation columns can be traced back to the end of the last century, when Yianatos studied the residence time distribution of radioactive tracer gases in flotation columns using the pulse response method [17]. Subsequently, Ityokumbul proposed a non-iterative program for estimating the bubble size in flotation columns [18,19]. In addition, Gorain has developed an empirical model of bubble surface area flow in a mechanical flotation cell by using a large number of industrial-scale pilot projects [20]. Sarhan proposed a computational fluid dynamics (CFD) model to study gas holdup and bubble fluid dynamics in a three-phase flotation column [21]. Wang also used CFD to model the flotation process in detail [22]. Ravichandran optimized the gas parameters to increase gas retention for better flotation performance [23]. Ravichandran optimized the gas parameters to increase gas retention for better flotation performance.

Bubble shape mainly depends on five physical parameters (diameter, velocity, density, viscosity, and surface tension), and the state description of bubble shape is mainly based on several dimensionless numbers, such as the Otworth number (Eo), the Weber number (We), the Reynolds number (Re), and the Morton number (Mo) [24,25]. The aspect ratio of bubbles is a very direct way to characterize the shape of bubbles, that is, the ratio of the short axis to the long axis of the bubble. In the past few years, scholars have conducted a great deal of research on the shape of single bubbles. Experimental research shows that the shape of bubbles can be accurately described by dimensionless numbers [26,27]. However, Los [28] pointed out that extending the experimental results of a single bubble to two-phase or multiphase flows under other flow conditions is a problem because the liquid flow conditions, phase properties, and bubble interactions will inevitably affect the shape of the bubble. Liu et al. [25] discovered that the aspect ratio of bubbles tends to stabilize as the bubble diameter increases, rather than following the inverse of the bubble diameter predicted by the correlation equation derived from single-bubble experiments. Bessani and Inzoli [29] discussed the inevitable relationship between bubble shape and specific operation conditions in the bubble cluster.

In this study, a three-phase fluidized bed is used as a new type of flotation column for mineral separation. Uniform energy dissipation in the fluidized bed improves the collision efficiency of mineral particles with gas bubbles, increasing energy utilization and the recovery of fine-grained minerals. The objective of this work is to study the effect of particle nature, filled bed height (H_0), gas velocity (V_g), and water velocity (V_l) on bubble diameter in TFC in the mineralized zone. The conclusions of this study are expected to optimize the operating parameters of the flotation mineralization process, enrich the study of three-phase fluidized bed flotation columns, and provide a reference for future research and design of TFC. It also provides on-site data references for the wide application of three-phase fluidized bed flotation columns in modern industrial production.

2. Materials and Methods

2.1. Material Preparation

The fluidized bed flotation column, as illustrated in Figure 1, consists of three interconnected components: the fluidized mineralization section, foam selection area, and media ore circulation system. These components operate in synergy according to the following functional principle: a rising water flow passes through and interacts with the filling particles within the mineralization and fluidization sections. Gradually, these particles become fluidized, forming a turbulent and porous layer known as a fluidized bed. Gas generated by the gas compressor at the bottom of the tower gas distributor (ceramic plate) is then released into this bed as bubbles of a specific diameter. Simultaneously, stirred slurry is pumped from the bottom of the flotation column using circulating water propelled by a circulating pump. As this slurry rises within the column, it encounters both gas bubbles and turbulence-controlled particles present within the fluidized bed layer. Under their combined influence, collision-induced mineralization takes place. By adjusting parameters such as apparent water flow rate and particle characteristics, turbulence intensity within this layer can be modulated to ensure sufficient mineralization for particles with varying granularities. Mineralized bubbles are subsequently transported to an expanded cross-sectional area in the column flotation section, where they undergo further mineralization due to prolonged flotation time before ultimately yielding flotation concentrate—a process that effectively separates mineralization from flotation.

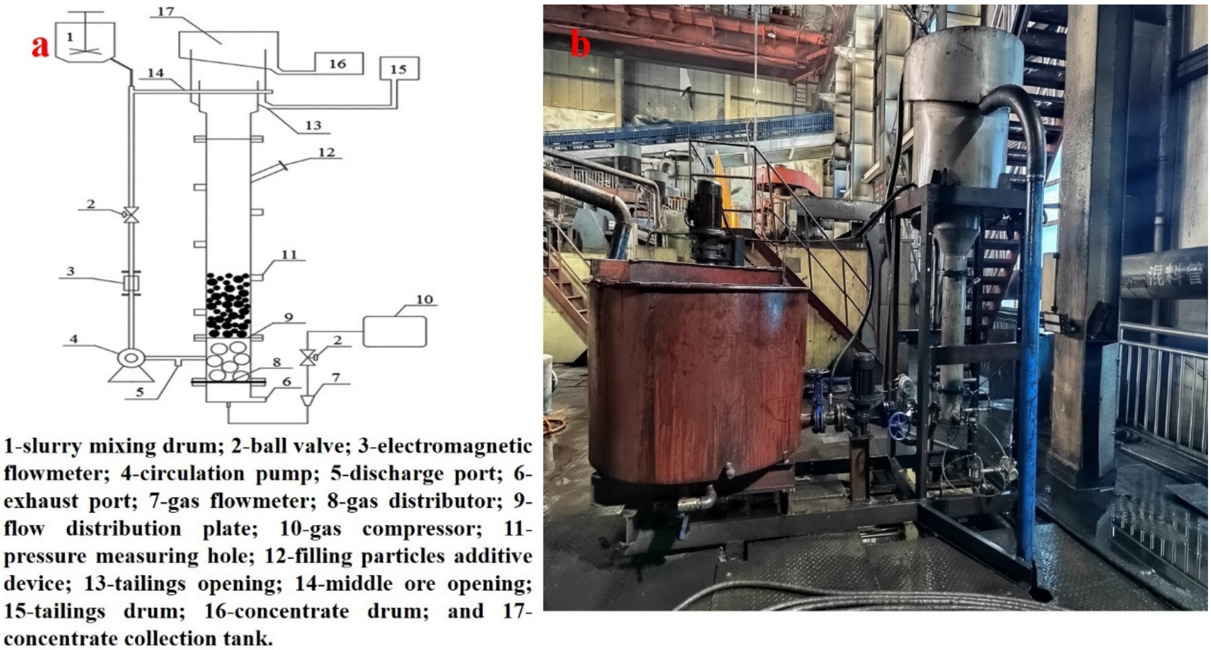

Figure 1. (**a**) Schematic diagram of the laboratory scale. (**b**) Schematic of the full-size equipment.

The semi-industrial test of a horizontal filling medium flotation column was carried out at Henan Shenhuo Group Co. The specifications of the flotation column were Φ200 × 2680, and the whole body was made of iron. At the beginning of the test, a portion of coal slurry cyclone concentrate was first intercepted by a slurry mixing bucket, and the chemicals were added to a 2 m^3 slurry mixing bucket. Then, pump the slurry flotation column for the column flotation test to be stable after the work of the equipment was intercepted. Concentrate samples and tailings samples were added to the ore samples in the slurry barrel to add the chemicals before the interception. Air and water flow control distribution through the air rotor flowmeter and water rotor flowmeter and the corresponding manual adjustment valve to achieve the apparent speed of the slurry by changing the size of the discharge caliber at the bottom of the flotation column. Throughout this paper, gas and liquid velocities are expressed as superficial velocity and superficial liquid velocity, respectively. The properties of the solid particles in the experiment are shown in Table 1, and the solid particles used were steel balls A, if not otherwise specified.

Table 1. Properties of solid particles.

Filling Particle	Calibre (mm)	Densities (kg/m^3)
Glass bead A	3.00	2698
Glass bead B	4.00	2698
Glass bead C	5.00	2698
Ball bead A	3.00	7800
Ball bead B	4.00	7800
Ball bead C	5.00	7800

2.2. Experiment Methods

As shown in Figure 2, the bubble parameters of this experiment are mainly obtained by the BVW-2 multichannel conductance probe bubble characteristic parameter measuring instrument. When measuring, the conductance probe is placed in the gas-liquid two-phase flow, the two conductance probes of the same measuring channel are arranged along the direction of bubble movement, and the probes apply an alternating voltage signal generated by the signal excitation source. When the bubble moves upward, the probe pierces the same bubble, and the conductivity value at the tip of the probe changes, which can be adjusted by detection, amplification, and level. The conductivity values are collected by the computer and converted into the corresponding bubble parameters.

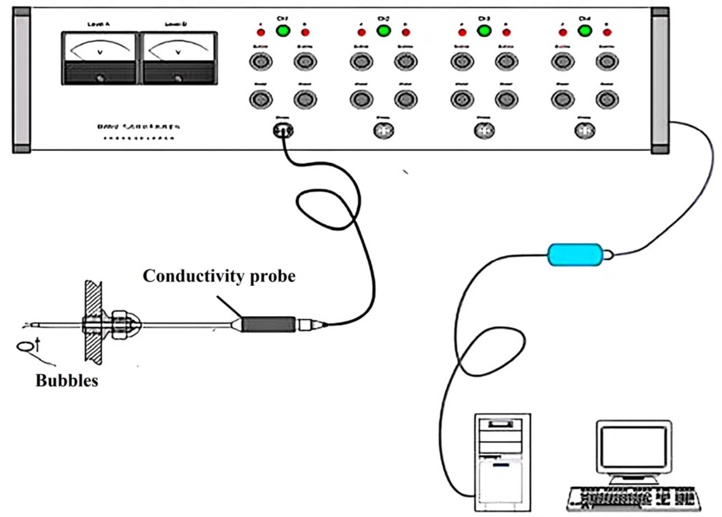

Figure 2. Equipment contact diagram for BVW-2.

3. Results and Discussion

3.1. Study of the Effect of Particle Properties on Bubble Diameter

The properties of the turbulence-regulating particles determine the bubble parameters in the mineralized zone to some extent. In view of this, we will explore the applicability of different filling particles and arrange the follow-up experiments accordingly. In this section, the first study is the variation of bubble diameter when different particles are used as filling materials. Figure 3 represents the variation of bubble diameter with apparent air velocity when solid-phase particles with different densities and particle sizes are used as filling materials for a certain initial static bed height (total mass of solid-phase particles) and apparent water velocity. In order to clearly distinguish the effect of different materials on the bubble diameter, the large-density steel beads and small-density glass beads are reseated separately, with the diameter of 3 mm steel beads represented in both figures. The purpose is to use 3 mm steel beads as a comparison term to better distinguish the effect of two materials on the experimental results. As can be seen from Figure 3a, when the particle size is the same and the density of the steel beads as the filling particles is small, the bubble diameter generated in the fluidized bed is small, and with the increase of the apparent gas velocity, the magnitude of the bubble change is small. After calculations, we learned that in the experimental study of the parameter range, the change in the bubble diameter will not be more than 15%. Glass beads with the same particle size will produce larger bubbles under the same experimental conditions. With the increase in apparent gas velocity, the bubble will increase. The apparent gas velocity increases and increases, and the bubble diameter changes in a larger range. The bubble is difficult to change in a relatively stable range, and the magnitude of change is more than 50%. The above analysis shows that under the same experimental conditions, the bubbles produced when using high-density steel balls as filler particles are smaller, and the change of bubbles will change in a relatively small range.

As can be seen from Figure 3b, when glass beads A, B, and C of the same material are used as filler particles, the bubble diameter increases with the increase in superficial gas velocity, and under the same experimental conditions, the larger the particle size of filler particles, the larger the bubble diameter generated in the fluidized bed.

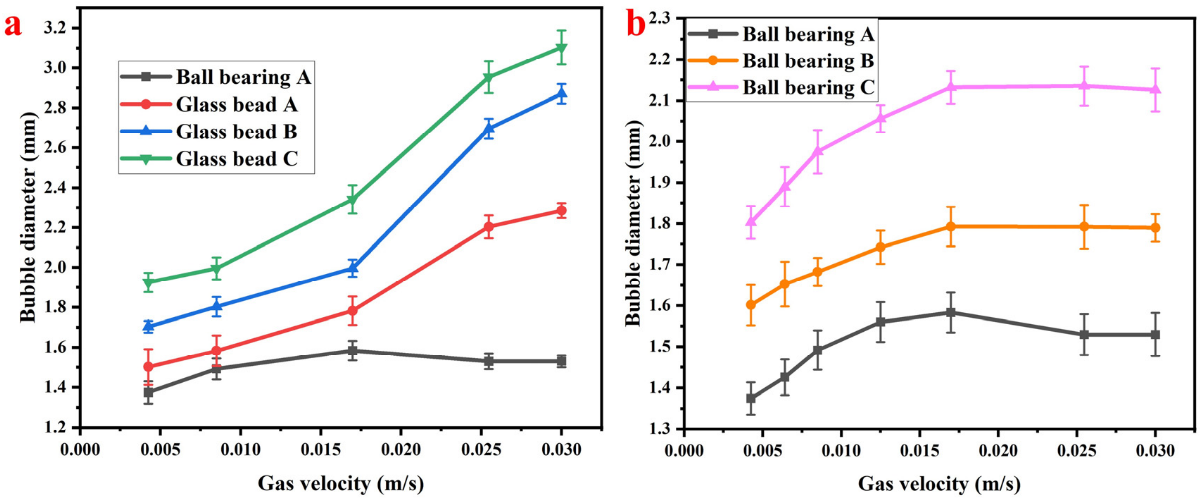

Figure 3. (**a**) Relationship between laboratory-scale particle properties and bubble diameter. (**b**) Relationship between particle properties and bubble diameter for a full-size device. (H_0 = 0.262 m, V_1 = 0.169 m/s).

After the above analysis, it can be seen that, on the one hand, when the particle size is the same, the density of the particles as a filling material when the bubble diameter is small, and the bubble will be in a relatively small range of change, while the density of the particles as a filling material generated by the bubble diameter is relatively large, and bubbling changes in the magnitude of the larger bubble, the bubble is unstable. On the other hand, when the density is the same, the bubble diameter produced in the fluidized bed increases with the increase in particle size of the packed particles.

The main reason for the first phenomenon can be analyzed as the reason for the change in bubble diameter. Cho [29] pointed out that the change in bubble diameter in multiphase flow is mainly caused by the coalescence of small bubbles and the rupture of large bubbles. The change in bubble diameter is actually a dynamic balance of the two effects; when the coalescence effect is greater than the rupture effect, the average diameter of the bubble group tends to increase; when the rupture effect is greater than the coalescence effect, the average diameter of the bubble group tends to decrease. Filling the same particle size particles, due to the greater density of steel beads, fluidized bed to reach the fluidized state by the interference of steel beads settlement rate is greater, the fluidized bed of larger diameter bubbles for shear and destruction of the role of the stronger, larger diameter bubbles in the steel beads of the shear and destruction of the action of the formation of a number of smaller diameter bubble group, this is the same conclusion as Allan's study [30]. However, due to the density of glass beads is small, in the fluidized bed to reach the end point of the fluidization of the glass beads of on the contrary, due to the small density of glass beads, after reaching the end point of fluidization in the fluidized bed, the settling velocity of the glass beads is low, and the bubble clusters exhibit a decreasing average diameter trend.

The main reason for the second phenomenon (take the steel ball as an example) is that the density is the same, but the particle size is different. On the one hand, according to the relevant formula, the interference of the filling particles at the end of the rate of sedimentation increases (4 mm, an increase of 18.9%; 5 mm, an increase of 35.5%), increasing the shear on the large-diameter bubbles, which belongs to the "qualitative" role of the effect. On the other hand, when the density is the same under the same height of the static bed, the number of static bed-filled particles of large particle size is less than the number of particles in the static bed of small particle size. The larger the number of particles in the static bed, the more filled particles play a role in the shear destruction of the bubbles, which belongs to the "quantitative" effect of shear. According to the experimental results, it can be seen that in the case of the same density and different particle sizes, the effect of filling bubbles with particles is greater than the effect of "quantity" or "quality."

3.2. Study of the Effect of Particle Bed Height on Bubble Diameter

In fluidized bed flotation columns, the static turbulent particle height can prolong the residence time of gas bubbles inside the column and increase the contact area of the gas-liquid-solid three-phase interface. The purpose of this test is to investigate the effect of static turbulent particle height on the bubble diameter in the mineralized area within the fluidized bed flotation column in order to find a suitable static turbulent particle height. The specific test results are shown in Figure 4.

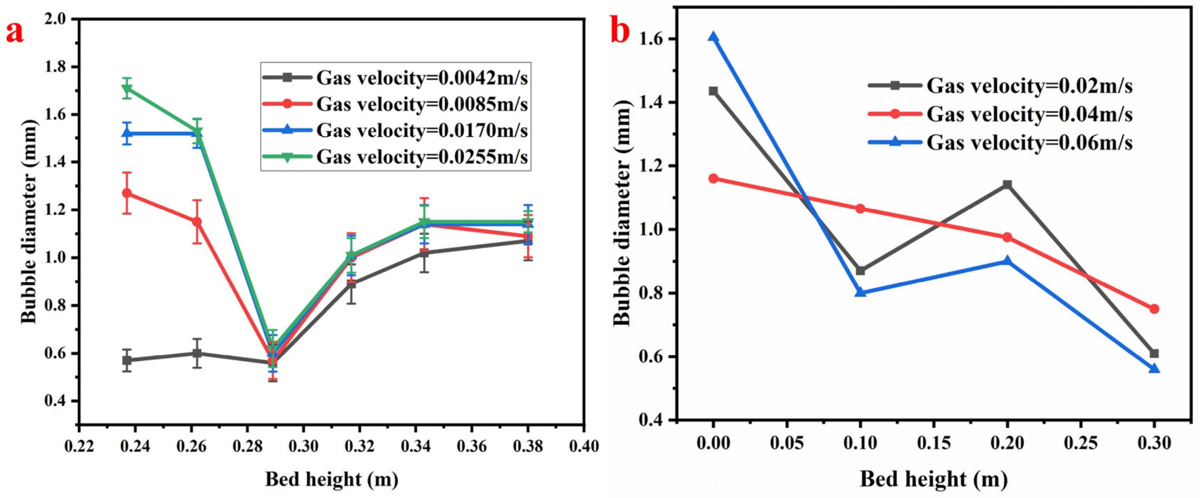

Figure 4. (**a**) Relationship between height of laboratory-scale particle bed and bubble diameter. (**b**) Relationship between particle bed height versus bubble diameter for a full-size facility (V_1 = 0.226 m/s).

From Figure 4a, it can be observed that at different static turbulent particle heights and at the same gas velocity, the bubble diameter shows a tendency to decrease and then increase with the increase in the height of the packing layer. In addition, at the same gas velocity, it can be seen that the bubble diameter is the smallest when the height of the stationary turbulent particles is 0.289 m. This is mainly due to the fact that with the increase in the height of the stationary turbulent particles, the shear effect of the packing particles on the bubbles is strengthened, which prolongs the time for the bubbles to pass through the stationary turbulent particles. When the height of stationary turbulent particles reaches a certain level, the shearing effect reaches its optimum, and then the shearing effect decreases. In this process, bubble coalescence occurs inside the bed due to the prolonged time of bubble overflow, resulting in an increase in bubble diameter at higher stationary turbulent particle heights instead.

Meanwhile, from the curve analysis in Figure 4a, it can be seen that under different air velocities, with the increase in the height of stationary turbulent particles, the change in bubble diameter is very small, especially when the height of stationary turbulent particles is between 0.343 m and 0.380 m. The bubble diameter basically stays unchanged with the increase in air velocity. This further proves that the height of stationary turbulent particles has both an obvious shear effect on bubble diameter and an obvious effect on bubble coalescence. When the shearing effect exceeds the coalescence effect, the packing layer has a shearing effect on the bubbles. On the contrary, when the packing layer height is too high, the coalescence effect will be significantly stronger than the shear effect, but this helps to homogenize the bubble distribution at higher gas velocities. Therefore, it can be assumed that selecting a higher height of static turbulent particles is beneficial to improving the effect of bubbles in the mineralized region.

In industrial testing, as you can see from Figure 4b, when the water velocity is 0.2 m/s, the bubble diameter decreases with the increase in the static turbulent particle height at the four gas velocities of 0.02 m/s, 0.04 m/s, and 0.06 m/s, and then increases. It can be seen that for the three gas velocities, the bubble diameter reaches its minimum value at a height of 0.3 m. The reason for this phenomenon is that the initial increase in the height of static turbulent foam particles prolongs the time of passing through the whole bed, the static height of turbulent particles continues to increase, and the shearing effect of foam-filled particles on the bed reaches its best effect. Then, the increase in the static height of turbulent particles weakens the shearing effect of foam-filled particles, and the bubble diameter increases again. At the same time, we can see that, at large static turbulent particle heights, especially at 0.2 m and 0.3 m, the bubble diameter corresponding to the four gas velocities changes very little. This indicates that the mass of the bed-filling body not only has a strong shearing effect on the bubbles but also has a strong merging effect on the bubbles in the bed. When the filling particles corresponding to the height of static turbulent particles have a greater shearing effect on the bubbles than their merging effect, the shearing effect occurs, which leads to a decrease in bubble diameter.

Based on the air velocity of 0.02 m/s, we measured the variation of bubble diameter with the height of stationary turbulent particles and water velocity, and it can be seen from Figure 5 that, for the three water velocities: 0.1 m/s, 0.15 m/s, and 0.2 m/s, the bubble diameter shows a tendency of decreasing and then increasing with the height of stationary turbulent particles at the gas velocity of 0.02 m/s. The bubble diameter is the smallest at the three liquid velocities and the smallest at the three liquid velocities. And it can be seen that for all three kinds of liquid velocities, the bubble diameter is minimized at the static turbulent particle height of 0.3 m. The bubble diameter of the liquid velocity is also minimized at the static turbulent particle height of 0.3 m. This is because when the filling height is small, the time for bubbles to pass through the bed is shorter, and the residence time inside the bed is shorter, which leads to fewer times for moving the bed to cut bubbles. At this time, the function of the bed is to prolong the residence time of bubbles in the bed and slow down the movement of bubbles. When the height of static turbulent particles continues to increase to 0.3 m, the particles filled with mineralized zone move upward to shear the water, and at this time, the shearing effect is the best, which shows that the diameter of water is the smallest. Then, the height of static turbulent particles increases, and the bubble diameter increases again. The reason for this phenomenon is that the bed filling height is too large so the bubbles through the bed can extend the time. When the bubble through the bed is easy due to the extension of time through the coalescence, the static turbulence particle height is higher, and the bubble diameter will have a slightly larger phenomenon. At the same time, we can see that the bubble diameter decreases with the increase in water velocity at the static turbulent particles at a large height, especially at 0.2 m and 0.3 m. This shows that the bed surface occupies most of the influencing factors when the water velocity increases. This is because when the water flow velocity increases, the particles in the bed are affected by the water flow velocity, and the movement velocity in the mineralized zone is accelerated, thus enhancing the shearing effect on the bubbles. When the bubble passes through the bed, the shearing effect on the bubble increases, and the diameter of the bubble decreases. In contrast, the change in the diameter of the bubbles does not change much when the water velocity increases, which is due to the fact that the water velocity occupies a large influence factor in the fluidized bed. The swallowing effect of the larger packed bed heights is greater than the shear effect, but this phenomenon is beneficial for the homogenization of the bubbles at large water flow velocities.

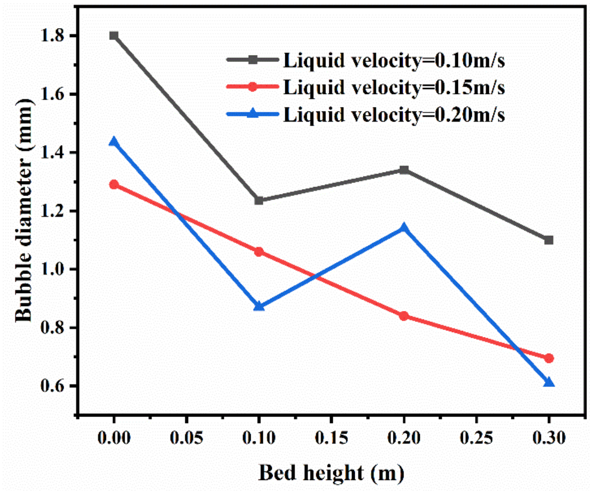

Figure 5. Bed height versus bubble diameter for water velocity (Vg = 0.02 m/s).

3.3. Study of the Effect of Gas Velocity on Bubble Diameter in the Mineralized Region

Under different water velocities, Figure 6a reflects the change in bubble diameter with gas velocities. It can be seen that the effect of gas velocity on bubble diameter shows different patterns of change under different operating water velocities. In the case of low water velocity (V_l = 0.170 m/s and V_l = 0.189 m/s), the bubble diameter is negatively correlated with the apparent gas velocity. The main reason is that the low apparent water velocity leads to low turbulence intensity of the liquid phase in the bed, and with the addition of the apparent gas velocity, the turbulence intensity of the liquid phase in the bed is increased, and there is synergy between the apparent gas velocity and the water velocity, and the shear effect of the steel beads on the bubbles is therefore enhanced. Therefore, the bubble diameter has a tendency to decrease all the time. That is, when the apparent water velocity is low, the increase in the gas phase is favorable to the reduction of the bubble diameter. With the increase in gas velocity, the bubble diameter gradually decreases. This is mainly due to the mild turbulence of the liquid phase at low water velocity. As the gas velocity increases, the turbulence of the gas and liquid phases is strengthened, and the addition of the gas phase makes the liquid phase turbulence become active, which promotes the shear effect of the particle-filled steel beads on the bubbles as well as the mixing effect of the liquid phase on the gas phase, resulting in a decrease in the bubble diameter. That is, at a lower water velocity, increasing the gas velocity will make the bubble diameter smaller.

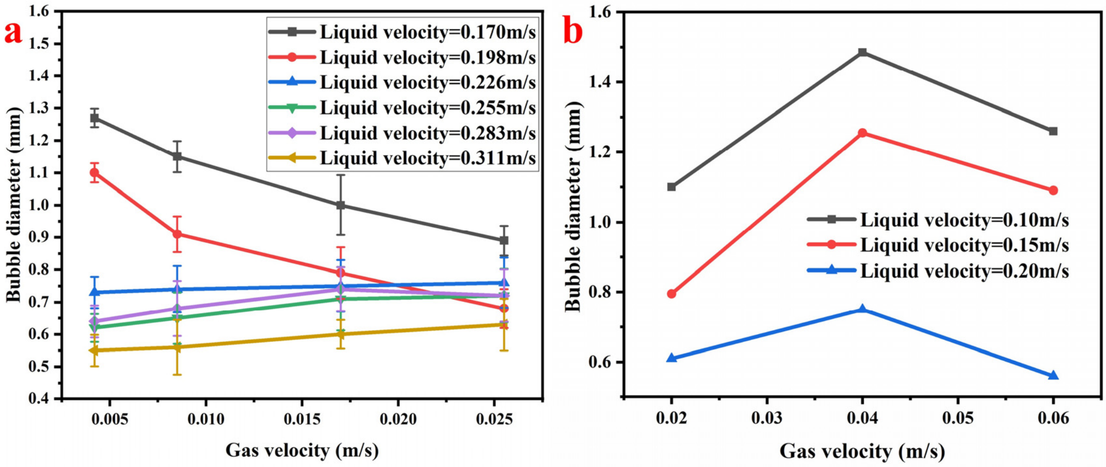

Figure 6. (**a**) Laboratory-scale gas velocity versus bubble diameter (H_0 = 0.289 m). (**b**) Relationship between gas velocity and bubble diameter for a full-size device (H_0 = 0.3 m).

However, at high water velocities (apparent liquid velocity greater than 0.226 m/s), it is observed that the bubble diameter basically tends to increase gradually with increasing gas velocities, although the increase is not significant. This is mainly because liquid-phase turbulence is more intense at high water velocities. Compared with the gas velocity conditions in this study, the effect of the liquid phase on the bubble diameter was more pronounced, while the addition of the gas phase had less effect on the liquid phase. In addition, usually, the effect of gas velocity on bubble diameter is decisive, so the bubble diameter tends to increase. However, in the case of high water velocity (V_l = 0.311 m/s), the bubble diameter did not change significantly with the change in gas velocity and basically remained unchanged. This confirms the above conclusion from another angle, that is, the effect of gas velocity on the bubble diameter within the mineralized region of the fluidized bed flotation column is not obvious in the case of intense liquid phase turbulence.

In addition, there is no uniform conclusion regarding the effect of gas velocity on bubble diameter size in the relevant references, which suggests that the role of gas velocity depends on the operating region and the specific system properties. The range of gas velocity in this experiment is 0.0042~0.0255 m/s, which belongs to the lower range of gas velocity adjustment, while the range of liquid velocity adjustment is wider, which is 0.170~0.311 m/s. In this case, the mineralized area of the fluidized bed flotation column is in the bubble dispersion and agglomeration zones. In the case of low water velocity, increasing the gas velocity exacerbated the gas-liquid two-phase turbulence, which enhanced the effect of bubble crushing, resulting in a decrease in the average bubble diameter.

As shown in Figure 6b, the bubble diameter with the increase in gas velocity has a certain trend of increase, but the increase is not obvious. The reason for this is mainly due to the higher water velocity of the liquid phase in the bed of the turbulence of the liquid phase, which strengthens the effect of the liquid phase and the water velocity on the bubble diameter of the liquid phase compared to the impact of the bubble diameter of the liquid phase on the bubble, which is more intense after adding the gas phase of the liquid phase. The effect of gas velocity on the bubble diameter in general plays an absolute role, so in the case of high water velocity, the bubble diameter will show a certain trend of increase. Under the condition of high water velocity, the increase in gas velocity will lead to the enhancement of the turbulence of gas-liquid two-phase in the bed and the enhancement of the shear effect on the bubbles, so the bubble diameter will be reduced.

3.4. Study of the Effect of Water Velocity on the Diameter of Bubbles in the Mineralized Region

The importance of water velocity within a flotation column is reflected in its effect on "static sorting" and turbulence regulation. This study of the effect of water velocity on bubble diameter and gas content in the mineralized zone of the column can be useful for subsequent industrial tests and for a better understanding of the flow regime in the mineralized zone of a fluidized bed flotation column.

From Figure 7a, it can be observed that with the increase in water velocity, the bubble diameter shows a trend of decreasing at first and then increasing at different gas velocities. In the case of higher water velocity, the bubble diameter remains basically unchanged. In other words, under the condition of low water velocity (less than 0.226 m/s), the bubble diameter gradually decreases with the increase in water velocity. This is mainly due to the fact that the increased water velocity enhances the turbulence intensity of the liquid phase on the one hand and provides enough kinetic energy for the steel balls to produce a stronger shearing effect on the bubbles on the other hand, so the bubble diameter gradually decreases [18]. This is mainly due to the increase in water velocity.

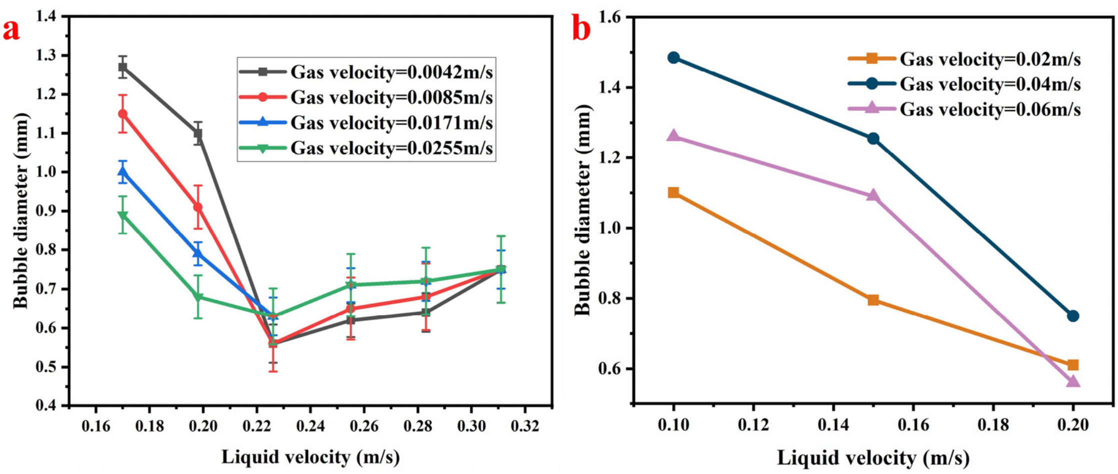

Figure 7. (**a**) Relationship between water velocity and bubble diameter at the laboratory-scale (H_0 = 0.289 m). (**b**) Relationship between water velocity and bubble diameter for full-size equipment (H_0 = 0.3 m).

When the apparent liquid velocity exceeds a certain value (0.226 m/s in this experiment), the increase in the apparent liquid velocity will not produce the above effect but will lead to an increase in the bubble diameter. This is because, although the increased apparent liquid velocity increases the turbulent intensity of the liquid phase and the kinetic energy of the particle-filled steel balls, it also increases the porosity between the steel balls, reduces the collision efficiency between the particle-filled steel balls, and weakens or even makes the shear effect ineffective. In this case, the bubble size in the mineralized zone of the fluidized bed flotation column only depends on the turbulent action of the liquid phase, so the bubble diameter tends to increase. In the lower water velocity, the turbohence intensity of the liquid phase is lower, the kinetic energy obtained by the steel ball is also lower, the shear effect of the steel ball on the bubble is weaker, so the bubble diameter is also larger, but the subsequent increase in apparent water velocity strengthens the turbalance intensity of the liquid phase, the gap turbulence intensity increases, the kinetic energy obtained by the steel ball is increased, and the bubbles floated up to the mineralized ara are subjected to enhanced shear frequency of the steel ball, so there is a trend to reduce the bubble diameter. The bubble diameter has a tendency to decrease until it is minimized. In addition, at high water velocity, the turbulence of the liquid phase is already very intense, and the bubble-breaking effect reaches its maximum. The bubble-breaking effect will not be significantly affected by increasing the liquid flow velocity. The intensity of liquid-phase turbulence is too large, which increases the porosity of steel balls and reduces the collision probability between the fluidized steel balls, resulting in insufficient shear rupture of bubbles. In this case, bubbles become smaller and more dependent on the turbulence of the fluid.

As can be seen from Figure 7b, when the height of the filled bed is 0.3 m, the bubble diameters of the three air velocities (0.02 m/s, 0.04 m/s, and 0.06 m/s) show a decreasing trend with the increase in water velocity. When the water velocity was 0.2 m/s, the bubble diameter corresponding to the three air velocities reached the minimum value. The main will—oneness of this phenomenon is that the increase of water velocity strengthens the turbo-hence intensity of the liquid phase in the whole system; and the increase of water velocity provides a larger kinetic energy to the steel balls in the bed; so that they have a strong shearing effect on the bubbles entering the bed in the whole movement of the bed; and so the bubble diameter gradually decreases in the stage of the increase of water velocity at the beginning.

4. Conclusions

In this study, a new type of three-phase fluidized flotation tower was investigated to determine the effect of relevant operating parameters on the bubble diameter within the mineralized environment. The specific conclusions are as follows:

(1) The selection of steel beads with high-end velocity of free settling and high density as filling particles has a stronger shearing effect on the bubbles in the mineralized flow field region, and the resulting bubble diameter is smaller.

(2) The increase in filling bed height has a very obvious reinforcing effect on the reduction of bubble diameter, and after the filling bed height reaches a certain value, the filling bed height will weaken the effect of apparent gas velocity on the bubble diameter.

(3) The apparent gas velocity has different effects on the bubble diameter. Under the condition of low water velocity, the increase in apparent gas velocity helps to reduce the bubble diameter. When the apparent water velocity is greater than 0.226 m/s, the effect of the apparent gas velocity on the bubble diameter is not obvious; the increase in apparent water velocity helps to reduce the bubble diameter. Obviously, when the apparent water velocity is greater than 0.226 m/s, the bubble diameter has a gradual increasing trend.

In this study, by comparing and analyzing the laboratory data of the three-phase fluidized flotation tower with the data of the industrial size, it is concluded that the gas parameters during the work at the industrial site are the same as those in the laboratory. It provides a real data reference for the industrial application of a three-phase fluidized bed flotation column in the future.

Author Contributions: Conceptualization, M.Y. and Y.L.; validation, T.Y.; investigation, M.Y. and N.H.; resources, N.H. and T.Y.; data curation, M.Y. and Y.L.; writing—original draft preparation, M.Y.; writing—review and editing, M.Y. and Y.L.; supervision, N.H.; project administration, M.Y.; funding acquisition, Y.L. All authors have read and agreed to the published version of the manuscript.

Funding: This research was financially supported by the Key Science and Technology Projects of China National Coal Group Corp. (20231CY003).

Data Availability Statement: The data are derived from our teamwork or references and are available.

Conflicts of Interest: Author Mao Yin was employed by the company Henan SUNHO Group Company Limited. The remaining authors declare that the research was conducted in the absence of any commercial or financial relationships that could be construed as a potential conflict of interest.

References

1. Jo, Y.B.; Park, S.H.; Yoo, H.S.; Kim, E.S. GPU-based SPH-DEM Method to Examine the Three-Phase Hydrodynamic Interactions between Multiphase Flow and Solid Particles. *Int. J. Multiph. Flow* **2022**, *153*, 104125. [CrossRef]
2. Jena, H.M.; Sahoo, B.K.; Roy, G.K.; Meikap, B.C. Characterization of hydrodynamic properties of a gas-liquid-solid three-phase fluidized bed with regular shape spherical glass bead particles. *Chem. Eng. J.* **2008**, *145*, 50–56. [CrossRef]
3. Abu Khalifeh, H.; Madhuranthakam, C.M.; Dhib, R. Empirical models for the hydrodynamics of turbulent bed contactor with non-Newtonian liquids: (Part 3). *Chem. Eng. Commun.* **2021**, *208*, 110–125. [CrossRef]
4. Venkatraman, P.Z. Evaluation of an Advanced Fine Coal Cleaning Circuit. Ph.D. Thesis, Virginia Polytechnic Institute and State University, Blacksburg, VA, USA, 1996.
5. Fan, M.; Tao, D.; Zhao, Y.; Honaker, R. Effect of nanobubbles on the flotation of different sizes of coal particle. *Miner. Metall. Process.* **2013**, *30*, 157–161. [CrossRef]
6. Bhunia, K.; Kundu, G.; Mukherjee, D. Statistical model for gas holdup in flotation column in presence of minerals. *Can. Metall. Q.* **2015**, *54*, 235–246. [CrossRef]
7. Lei, W.; Zhang, M.; Zhang, Z.; Zhan, N.; Fan, R. Effect of bulk nanobubbles on the entrainment of kaolinite particles in flotation. *Powder Technol.* **2020**, *362*, 84–89. [CrossRef]
8. Cai, X.; Chen, J.; Liu, M.; Ji, Y.; An, S. Numerical studies on dynamic characteristics of oil-water separation in loop flotation column using a population balance model. *Sep. Purif. Technol.* **2017**, *176*, 134–144. [CrossRef]
9. Li, Y.R.; Li, Q.; Yang, J.M.; Zhou, X.M.; Yin, X.M.; Zhao, D.M. Expression patterns of Doppel gene in golden hamster: Quantification using real-time RT-PCR. *Mol. Cell. Probes* **2008**, *22*, 255–258. [CrossRef]
10. Vadlakonda, B.; Mangadoddy, N. Hydrodynamic study of three-phase flow in column flotation using electrical resistance tomography coupled with pressure transducers. *Sep. Purif. Technol.* **2018**, *203*, 274–288. [CrossRef]

11. Han, J.; Fang, J.; Yang, T.; Chen, P.; Liu, T.; Li, Y. Particle motion analysis of a new three-phase fluidized bed flotation column with glass sphere particles. *Adv. Powder Technol.* **2023**, *34*, 104265. [CrossRef]
12. Sobrino, C.; Almendros-Ibáñez, J.A.; Santana, D.; Vázquez, C.; De Vega, M. Maximum entropy estimation of the bubble size distribution in fluidized beds. *Chem. Eng. Sci.* **2009**, *64*, 2307–2319. [CrossRef]
13. Lefebvre, S.; Guy, C.; Chaouki, J. Solid phase hydrodynamics of three-phase fluidized beds—A convective/dispersive mixing model. *Chem. Eng. J.* **2007**, *133*, 85–95. [CrossRef]
14. Jena, H.M.; Roy, G.K.; Meikap, B.C. Prediction of gas holdup in a three-phase fluidized bed from bed pressure drop measurement. *Chem. Eng. Res. Des.* **2008**, *86*, 1301–1308. [CrossRef]
15. Wang, T.; Wang, J.; Yang, W.; Jin, Y. Experimental study on bubble behavior in gas-liquid-solid three-phase circulating fluidized beds. *Powder Technol.* **2003**, *137*, 83–90. [CrossRef]
16. Han, N.; Gao, R.; Peng, H.; He, Q.; Miao, Z.; Wan, K. Selective recovery of lithium ions from acidic medium based on capacitive deionization-enhanced imprinted polymers. *J. Clean. Prod.* **2022**, *373*, 133773. [CrossRef]
17. Yianatos, J.; Vinnett, L.; Panire, I.; Alvarez-Silva, M.; Díaz, F. Residence time distribution measurements and modelling in industrial flotation columns. *Miner. Eng.* **2017**, *110*, 139–144. [CrossRef]
18. Pan, H.; Li, Y.; Li, N.; Gao, F.; Fu, X.; Zhu, R.; Evans, G. Study on gas holdup in a fluidized flotation column from bed pressure drop. *Energy Sources Part A-Recovery Util. Environ. Eff.* **2018**, *40*, 1693–1700. [CrossRef]
19. Zhang, Z.; Fang, J.; Jing, L.; Li, Y. The separation of fine minerals in the synergy between the vertical fluidization section and inclined channels of the reflux classifier. *Asia-Pac. J. Chem. Eng.* **2023**, e2986. [CrossRef]
20. Gorain, B.K.; Franzidis, J.P.; Manlapig, E.V. The empirical prediction of bubble surface area flux in mechanical flotation cells from cell design and operating data. *Miner. Eng.* **1999**, *12*, 309–322. [CrossRef]
21. Sarhan, A.R.; Naser, J.; Brooks, G. CFD analysis of solid particles properties effect in three-phase flotation column. *Sep. Purif. Technol.* **2017**, *185*, 1–9. [CrossRef]
22. Wang, G.; Ge, L.; Mitra, S.; Evans, G.M.; Joshi, J.B.; Chen, S. A review of CFD modelling studies on the flotation process. *Miner. Eng.* **2018**, *127*, 153–177. [CrossRef]
23. Ravichandran, V.; Eswaraiah, C.; Sakthivel, R.; Biswal, S.K.; Manisankar, P. Gas dispersion characteristics of flotation reagents. *Powder Technol.* **2013**, *235*, 329–335. [CrossRef]
24. Ellingsen, K.; Risso, F. On the rise of an ellipsoidal bubble in water: Oscillatory paths and liquid-induced velocity. *J. Fluid Mech.* **2001**, *440*, 235–268. [CrossRef]
25. Liu, L.; Zhang, H.; Yan, H.; Ziegenhein, T.; Hessenkemper, H.; Zhou, P.; Lucas, D. Experimental studies on bubble aspect ratio and corresponding correlations under bubble swarm condition. *Chem. Eng. Sci.* **2021**, *236*, 116551. [CrossRef]
26. Aoyama, S.; Hayashi, K.; Hosokawa, S.; Tomiyama, A. Shapes of ellipsoidal bubbles in infinite stagnant liquids. *Int. J. Multiph. Flow* **2016**, *79*, 23–30. [CrossRef]
27. Lehr, F.; Millies, M.; Mewes, D. Modelling of breakage rate and bubble size distribution in bubble columns accounting for bubble shape variations. *Chem. Eng. Sci.* **2018**, *187*, 391–405.
28. Loth, E. Quasi-steady shape and drag of deformable bubbles and drops. *Int. J. Multiph. Flow* **2008**, *34*, 523–546. [CrossRef]
29. Besagni, G.; Inzoli, F. Bubble sizes and shapes in a counter-current bubble column with pure and binary liquid phases. *Flow Meas. Instrum.* **2019**, *67*, 55–82. [CrossRef]
30. Gomez-Flores, A.; Heyes, G.W.; Ilyas, S.; Kim, H. Prediction of grade and recovery in flotation from physicochemical and operational aspects using machine learning models. *Minerals Eng.* **2022**, *183*, 107627. [CrossRef]